Strategic Deployment of Battery Swapping Cabinets for Phase Balancing in Low-Voltage Distribution Network

Bongkoj Sookananta† and **Mongkol Pusayatanont**, Non-members

ABSTRACT

The growing integration of low-carbon technologies (LCTs), particularly electric vehicles (EVs), has intensified phase imbalance in low-voltage distribution networks due to the uneven distribution of single-phase loads. This leads to voltage unbalance, elevated neutral currents, and increased power losses, affecting network stability and efficiency. This study explores the deployment of battery swapping cabinets (BSCs) as a non-intrusive solution to mitigate these issues. Unlike conventional phase-balancing techniques, BSCs dynamically manage charging operations without service disruptions. However, findings indicate that BSCs primarily operate in charging mode, with limited discharging due to operational constraints and service demand patterns. A stochastic optimization framework integrating Stochastic Dual Dynamic Programming (SDDP) and Monte Carlo Simulation (MCS) is developed to optimize BSC placement and energy management. Evaluating a 104-bus low-voltage network in northeastern Thailand, results show that optimized BSC deployment reduces the Voltage Unbalance Factor (VUF) by up to 30.47%, improving grid performance. The study highlights the role of BSC energy management in load balancing. These findings underscore the potential of BSCs as grid-supporting infrastructure, enhancing network resilience while reducing phase imbalance.

Keywords: Battery swapping cabinet (BSC), voltage unbalance factor (VUF), stochastic optimization, electric vehicle (EV), low-voltage distribution network, energy management

1. INTRODUCTION

The rapid adoption of low-carbon technologies (LCTs), such as photovoltaic (PV) systems and electric vehicles (EVs), has transformed modern distribution networks, introducing new challenges in maintaining phase balance and voltage stability. The proliferation of single-phase EV chargers and residential PV systems disrupts traditional three-phase network architectures, leading to voltage unbalance, increased power losses, and excessive neutral currents, which degrade grid efficiency and reliability [1]. Addressing these issues requires innovative phase-balancing strategies that can dynamically adapt to modern, decentralized distribution networks.

Existing solutions, such as network reconfiguration, aim to reduce voltage deviations and power losses in multi-phase distribution systems [2]. However, these methods often involve load adjustments that risk service interruptions, making them impractical for real-time applications [3]. In contrast, EV charging management has emerged as a promising alternative, using optimization techniques to minimize the Voltage Unbalance Factor (VUF) by adjusting charging states, connection phases, and power ratings [4]. Advanced methods, such as glowworm swarm optimization (GSO) integrated with dynamic voltage restorer (DVR) units and PV systems, have been shown to improve voltage quality in unbalanced networks [5]. Additionally, coordinated charging models for residential plug-in hybrid EVs (PHEVs) optimize charging patterns, reducing unbalance in residential networks [6].

Despite these advancements, most research focuses on residential EV charging, neglecting the increasing demand for public battery-swapping infrastructure. The COVID-19 pandemic dramatically accelerated food delivery services, leading to a surge in electric two-wheelers such as e-bikes and e-scooters. In Singapore, 60% of food delivery riders joined the gig economy during the pandemic [7], with similar growth observed in China and Thailand. Even post-pandemic, food delivery remains a dominant sector, sustaining high electricity demand for EV charging [8]. This surge underscores the urgent need for scalable battery-swapping solutions to support growing delivery fleets while mitigating grid instability.

This research proposes battery swapping cabinets (BSCs) as an adaptive phase-balancing mechanism to stabilize distribution networks. Unlike conventional charging, BSCs dynamically manage charging loads and selectively discharge to counteract network imbalances. By integrating stochastic optimization techniques, including Monte Carlo simulations (MCS) [9] and stochastic dual dynamic programming (SDDP) [10], this study optimizes BSC placement and operation to enhance

Manuscript received on May 10, 2025; revised on May 26, 2025; accepted on June 1, 2025. This paper was recommended by Associate Editor Chainarin Ekkaravarodome.

The authors are with Department of Electrical and Electronics Engineering, Faculty of Engineering, Ubon Ratchathani University, Ubonratchathani, Thailand.

†Corresponding author: bongkoj.s@ubu.ac.th

Digital Object Identifier: 10.37936/ecti-eec.2525232.257979

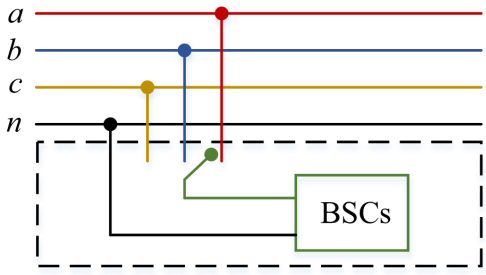

***Fig. 1**: BSCs Connection to LV Distribution Network.*

power quality and phase balancing under fluctuating load conditions.

The findings of this research provide a scalable framework for integrating BSCs into smart distribution grids, ensuring stable and resilient EV infrastructure while addressing the challenges posed by growing EV penetration and urban electrification. This study bridges the gap between public EV infrastructure and grid stability, advancing smart-grid-compatible energy solutions for future distribution networks.

The key contributions of this study are outlined as follows:

- This study proposes a bi-level optimization strategy for the placement and operation of BSCs to enhance phase balancing and minimize neutral current losses in low-voltage distribution networks.
- A stochastic optimization framework is developed by integrating SDDP with MCS to account for uncertainties in EV battery swapping demand and household energy consumption.
- A dynamic energy management strategy is introduced to coordinate operations between utility operators and BSC service providers, ensuring stable and efficient network performance.
- A sensitivity-driven optimization approach is implemented to maximize the effectiveness of phase balancing while preserving the primary function of BSCs as EV service infrastructure.
- A loadability margin constraint is incorporated to prevent network overloading, ensuring that selected BSC locations can handle power exchange within operational limits.

2. PROBLEM DESCRIPTION

The increasing integration of single-phase loads, particularly electric vehicle (EV) chargers, has intensified phase imbalance issues in low-voltage distribution networks, resulting in voltage unbalance, elevated neutral currents, and increased power losses in the neutral conductor. While battery swapping cabinets (BSCs) are emerging as critical infrastructure for electric mobility, their potential to mitigate phase imbalance remains underutilized.

This research addresses the optimal deployment and operation of Battery Swapping Cabinets (BSCs) to reduce voltage unbalance and neutral current, thereby enhancing overall network efficiency. As illustrated in Figure 1, each BSC is connected to a three-phase low-voltage (LV) distribution network through a selector switch. It is assumed in this study that the selector switch is controllable, enabling the phase of connection to be dynamically adjusted in response to real-time network conditions. The operating mode (charging or discharging) is managed separately based on network requirements. By strategically optimizing BSC placement, phase allocation, and operational scheduling, the proposed framework aims to minimize the voltage unbalance factor (VUF) and neutral conductor losses. The optimization considers key decision variables, including the bus location for cabinet installation, selected phase connection, operating mode, and charging/discharging power, all of which are coordinated to improve system performance under uncertainty.

Building upon this framework, the primary objective of the proposed approach is to improve network performance by mitigating voltage unbalance and neutral current, which directly contribute to power losses in LV distribution systems. Through optimal configuration and operation of BSCs, this study explores their role as a grid-supporting asset, enhancing the stability and efficiency of low-voltage distribution networks. The optimization problem can be expressed as:

$$\text{Minimize} \quad f(x) = VUF + P_N \tag{1}$$

The voltage unbalance factor, expressed as a percentage, is given by:

$$VUF = \frac{\max\left(\left|V_{an} - V_{avg}\right|, \left|V_{bn} - V_{avg}\right|, \left|V_{cn} - V_{avg}\right|\right)}{V_{avg}} \tag{2}$$

with the average phase voltage magnitude calculated as:

$$V_{avg} = \frac{\left|V_{an}\right| + \left|V_{bn}\right| + \left|V_{cn}\right|}{3} \tag{3}$$

The neutral line power losses (P_N) are defined as:

$$P_N = \sum_{l=1}^{N_{br}} I_{N,l}^2 R_{N,l} \tag{4}$$

where VUF is the voltage unbalance factor, representing the degree of voltage asymmetry across the three phases, x are variables including power charging or discharging from BSC and operational phase of connection, V_{an}, V_{bn}, and V_{cn} are phase A, B, C voltage magnitude, V_{avg} is the average of phase voltage magnitude, P_N is the total power losses in neutral lines, $I_{N,l}$ is current flow in neutral line l, which is caused by the imbalance in phase loading, and $R_{N,l}$ is the resistance of neutral line l.

The operation of the distribution network is subject to constraints that include power balance, bus voltage limits, and line thermal limits. The power balance constraint is expressed as:

$$P_{grid} + P_{DG} = P_{load} + P_{losses} \pm P_{BSC} \tag{5}$$

The power balance is evaluated using the calculation of unbalanced power flow in a four-wire distribution network [11], which accounts for the asymmetry in phase voltages and currents due to single-phase loads and BSC operations. This approach ensures a realistic assessment of network conditions, considering the impact of neutral current flow, voltage unbalance, and phase load distribution on system stability.

The bus voltage and thermal limits are expressed as:

$$V_i^{min} \leq V_i \leq V_i^{max} \tag{6}$$

$$I_l \leq I_l^{max} \tag{7}$$

where P_{grid} is the power supplied by the grid, P_{DG} is the power from distributed generation sources, P_{load} is the total power demand in the network, P_{losses} represents power losses in the network, P_{BSC} is the power from the BSCs, where $P_{BSC} > 0$ in charging mode and $P_{BSC} < 0$ in discharging mode, V_i^{min} and V_i^{max} represent the minimum and maximum allowable voltages at bus i, respectively, I_l is the current through line l, I_l^{max} is the maximum allowable current for line l.

The battery swapping cabinet operation constraints include the battery state and charging limits, the BSC capacity and slot capacity.

The charging and discharging power of a battery swapping cabinet is limited by its rated capacity and the capacity of individual slots. The total power exchanged with the distribution network depends on the combined available power of the batteries stored within the cabinet. The BSC operates in either charging or discharging mode based on the availability of reserved battery packs for electric vehicle EV services and the time of day. During off-peak periods, the BSC does not discharge power into the network due to low demand. Discharging is allowed only during peak hours, from 09:00 to 22:00. The operational constraints governing these modes are expressed as follows.

$$P_{BSC,t} = \begin{cases} \sum_{b=1}^{N_b} P_{b,t} - \sum_{b=1}^{N_{r,t}} P_{b,t}, & \text{if } N_{FB,t} \geq N_{r,t} \wedge t \in [9,22] \\ -\left| P_{BSC}^{\max} - \sum_{b=1}^{N_b} P_{b,t} \right|, & \text{otherwise} \end{cases} \tag{8}$$

$$P_{BSC} \leq P_{BSC}^{\max} \tag{9}$$

$$P_b \leq P_b^{\max} \tag{10}$$

where P_b represents the available power stored in the battery, sP_{BSC}^{max} and P_b^{max} are power rating of the battery swapping cabinet and the battery slot, N_b is the total number of battery slots in the BSC, N_{FB} represents the number of fully charged batteries in the BSC that are available and ready for EV service, $N_{r,t}$ is the minimum number of reserved batteries required at time t.

The state of charge (SOC) of the BSC must remain within predefined operational limits to ensure efficient charging and discharging cycles while preventing overloading or underutilization of the batteries. This constraint is expressed as:

$$SoC^{\min} \leq SoC \leq SoC^{\max} \tag{11}$$

where $SoC^{\min}$ and $SoC^{\max}$ represent the minimum and maximum allowable SoC levels of the BSC, ensuring that the batteries operate within safe and optimal ranges to prevent overcharging, deep discharging, or excessive degradation.

The change in the SoC of a battery within the BSC over a given time period is defined as:

$$\Delta SoC_{BSC,b} = \frac{\Delta t \left(P_{BSC,b}\right)}{W_{b,\max}} 100\% \tag{12}$$

where $\Delta SoC_{BSC,b}$ represents the percentage change in the SoC of battery over the time step, Δt is the time duration during which charging or discharging occurs, $W_{b,max}$ is the maximum charging or discharging energy that the battery b can handle within the time period t, $\eta\left(P_{BSC,b}\right)$ is the net power charge or discharging from the BSC depending of the charging/discharging efficiency of the battery.

$$\eta(P_{BSC,b}) = \begin{cases} \eta_c P_{BSC,b}, & P_{BSC,b} \geq 0 \text{ (charging mode)} \\ \frac{P_{BSC,b}}{\eta_d}, & P_{BSC,b} < 0 \text{ (discharging mode)} \end{cases} \tag{13}$$

where $P_{BSC,b}$ is the power associated with battery b in the battery swapping cabinet (BSC). It represents the power flowing into the battery when charging or out of the battery when discharging, η_c and η_d are charging and discharging efficiencies respectively and $\in (0, 1]$.

The updated SoC of battery b in the BSC at the next time step is given by:

$$SoC_{BSC,b,t+1} = SoC_{BSC,b,t} + \Delta SoC_{BSC,b} \tag{14}$$

However, when a battery is swapped at the end of a time step t, its SoC is replaced by that of the incoming battery from an electric vehicle (EV). This is expressed as:

$$SoC_{BSC,b,t+1} = SoC_{BSC,b,t}^{swap} \tag{15}$$

$SoC_{BSC,b,t}^{swap}$ is the SoC of the battery b that has been swapped by an EV at time t. This means that at the conclusion of time period t, the existing battery in the BSC is replaced by another battery brought in by the EV. The SoC of the newly swapped battery will be different from the previously stored battery, as it depends on the charge level of the battery arriving with the EV.

2.1 BSCs Placement

This study adopts a bi-level optimization framework for the strategic integration of battery swapping cabinets (BSCs) into low-voltage distribution networks. The first level of optimization focuses on determining the optimal locations for BSC deployment, ensuring an efficient

spatial distribution that mitigates phase imbalance. Once the locations are established, the second level optimizes both the power flow (charging or discharging) and the phase of connection for each BSC, aligning operational strategies with network performance objectives.

The BSC placement problem is formulated to maximize the sensitivity of the objective function with respect to variations in power drawn from or delivered to the distribution network. Since BSCs primarily serve EV battery-swapping needs, their operational impact on phase imbalance may vary. Therefore, this study aims to optimize their deployment to maximize their effectiveness in mitigating phase imbalance while fulfilling their primary function. This objective is mathematically expressed as follows:

$$\text{Maximize} \quad \frac{\partial f(x, \xi_s)}{\partial x_i} \tag{16}$$

$f(x, \xi_s)$ is defined in Equation (1) for each scenario $\boldsymbol{S}$, representing the optimization objective under stochastic variations in power demand within the distribution network. Monte Carlo Simulation (MCS) is employed to account for the uncertainties associated with EV charging demand and household electricity consumption, ensuring robustness in the BSC placement solution. This approach identifies locations where BSCs can provide the highest phase balancing benefits under fluctuating load conditions while adhering to network operational constraints.

Furthermore, the placement of BSCs must consider load-handling capability at each candidate location. To prevent network overloading, a loadability margin constraint is introduced, ensuring that the selected locations can accommodate the power absorption and delivery demands of BSCs. This constraint is expressed as:

$$P_{m,i} \geq P_{BSC}^{max} \tag{17}$$

The loadability margin [12] is given by:

$$P_{m,i} = \frac{V_{min} - V_i}{\frac{\partial V_i}{\partial P_i}} \tag{18}$$

where $P_{m,i}$ represents the maximum permissible power at bus i before violating voltage limits, $\frac{\partial V_i}{\partial P_i}$ is the voltage sensitivity coefficient with respect to active power changes, V_{min} is the minimum allowable bus voltage, V_i is the actual voltage at bus i

By incorporating both sensitivity-based optimization and loadability margin constraints, this approach ensures that BSC placement is both technically effective and operationally feasible, balancing phase unbalance mitigation with the network's capacity to handle power exchanges.

3. STOCHASTIC OPTIMIZATION

Stochastic optimization is a key approach for decision-making under uncertainty, widely used in power systems, energy management, and operational planning. Unlike deterministic methods, it incorporates probabilistic variations for more adaptive solutions. This research integrates Differential Evolution (DE), Monte Carlo Simulation (MCS), and Stochastic Dual Dynamic Programming (SDDP) to implement stochastic optimization effectively.

3.1 Differential Evolution

Differential Evolution (DE) is a stochastic optimization method designed for exploring optimal solutions in complex, nonlinear problems. While traditionally used for continuous optimization, its extension to discrete domains has proven effective for combinatorial and integer-based problems. This adaptability makes DE suitable for mixed-integer optimization in power systems [13]. By integrating customized mutation, crossover, and selection mechanisms, DE improves solution quality while maintaining constraint adherence. The detailed algorithmic structure of DE can be found in [14]. To accelerate the convergence of DE, the population size and number of search iterations can be reduced, ensuring a more computationally efficient optimization process while maintaining solution accuracy. Compared to other evolutionary techniques, DE achieves faster convergence due to its adaptive mutation and crossover mechanisms, which efficiently balance exploration and exploitation while requiring fewer function evaluations. This makes DE particularly suitable for applications involving a large number of scenarios, as it effectively navigates high-dimensional search spaces and optimizes complex stochastic problems with reduced computational overhead.

Due to its robust optimization capabilities, DE has demonstrated significant advantages over other heuristic techniques, such as Genetic Algorithms (GA) and Particle Swarm Optimization (PSO), particularly in terms of convergence speed, solution diversity, and ease of implementation [15]. Although advanced algorithms like the Many-Objective Marine Predators Algorithm (MaMPA) are well-suited for solving high-dimensional and many-objective optimization problems—especially in transmission-level Optimal Power Flow (OPF) [16] — their algorithmic complexity and higher computational burden may pose challenges for real-time applications and large-scale stochastic scenarios.

To address these constraints, this study employs a Mixed-Integer Differential Evolution (MIDE) approach, which offers a balance between computational efficiency and optimization accuracy. MIDE is particularly effective for problems involving both discrete and continuous decision variables, such as the strategic placement and energy scheduling of Battery Swapping Cabinets (BSCs) in low-voltage distribution networks. By treating parameters such as the number of buses, cabinet locations, and operational phases as discrete variables, and the power exchange between the grid and BSCs as continuous, MIDE efficiently explores complex search spaces under uncertainty. This makes it a practical and scalable

solution for integrating low-carbon technologies (LCTs) into future power systems.

3.2 Monte Carlo Simulation

Monte Carlo Simulation (MCS) is a probabilistic modeling technique designed to assess systems with inherent uncertainty by generating and evaluating multiple random scenarios [17]. A primary limitation of MCS is its requirement for a substantial number of scenarios to achieve statistically reliable outcomes, which can result in significant computational burden, particularly in large-scale or time-sensitive applications. Despite this, MCS remains highly suitable for problems characterized by uncertainty, as it offers a flexible and intuitive framework for capturing the probabilistic behaviour of input variables.

The MCS process begins with defining the problem and identifying key input variables that exhibit stochastic behaviours. In this research, these variables include fluctuations in load demand and BSC services. Once the sources of uncertainty are established, appropriate probability distributions are assigned based on historical data or expert knowledge, ensuring that the assigned distributions accurately reflect the characteristics of the data. The simulation then generates random samples from these distributions using statistical sampling techniques, creating multiple scenarios that capture different realizations of uncertainty.

Each generated scenario is processed through the system model to evaluate the relevant response variables, with the number of iterations determined by computational limitations and the desired accuracy of the results. To improve simulation accuracy, uncertainty in the estimated expectation decreases as the number of sampled scenarios increases, a concept known as the Standard Error of the Mean (SEM). Monte Carlo Simulation convergence is assessed using:

$$\frac{\sigma}{\sqrt{N_s}} \leq tol \tag{19}$$

where σ represents the standard deviation of the stochastic variables, N_s denotes the total number of sampled scenarios, tol is the predefined tolerance level for convergence assessment.

3.3 Stochastic Dual Dynamic Programming

Stochastic Dual Dynamic Programming (SDDP) [18] is a widely used optimization technique for multi-stage decision-making under uncertainty. One of its key limitations lies in its modelling and computational complexity, particularly when applied to large-scale or highly nonlinear systems, as it requires accurate value function approximations and dual-based formulations to ensure convergence. Nevertheless, SDDP remains highly effective for problems involving time-coupled decisions and uncertain system dynamics. It is particularly well-suited for applications in energy management, such as energy storage and demand-side operation, where sequential optimization over multiple stages is critical to system performance.

The effectiveness of SDDP in energy storage optimization has been demonstrated in large-scale applications, including hydrothermal scheduling, economic dispatch, and grid support. Studies highlight its ability to manage multiple services under uncertainty, optimizing storage for frequency regulation and energy allocation based on capacity and demand fluctuations [19]. A stochastic dynamic programming model has also been developed for co-optimizing storage in energy arbitrage and capacity support, emphasizing the need for adaptive scheduling in dynamic markets [20]. These insights align with BSC deployment, where dynamic charging and discharging are crucial for balancing EV service demand and maintaining grid stability.

The application of SDDP in this research involves a multi-stage decision-making process that optimally manages power consumption and delivery from BSCs while accounting for uncertainties in household electricity demand and EV charging patterns.

The process begins with defining the uncertain variables, including electricity demand and EV arrival rates, which are characterized using appropriate probability distribution functions (PDFs). At each stage of decision-making, multiple stochastic scenarios are generated to capture variations in these uncertainties. The SoC of each battery in the BSC is initialized, with stored energy levels determining the power available for discharge or required for charging. Constraints on charging and discharging power are imposed based on the allowable SoC range, ensuring operational feasibility.

A forward pass is conducted to simulate the decision-making process sequentially across all time steps. At each stage, the optimal decision variables are determined to minimize the cost function, which considers voltage unbalance mitigation and system operation constraints. The objective function is expressed as:

$$\text{Min } C\left(x_t, \xi_t\right) = f\left(x_t, \xi_t\right) + \alpha E\left(V_{t+1}\left(x_t, \xi_{t+1}\right)\right) \tag{20}$$

where $C\left(x_t, \xi_t\right)$ represents the total cost at time step t, which depends on the decision variables x_t, and the stochastic conditions ξ_t, $f\left(x_t, \xi_t\right)$ is the objective function related to phase unbalance mitigation, as described in Equation (1), evaluated at time t, $E\left(V_{t+1}\left(x_t\right)\right)$ denotes the expected cost-to-go, which is an expected future cost based on the optimal decision variables from the current stage, α is discounting factor, $\alpha \in (0, 1]$

$$V_{t+1}\left(x_t\right) = f\left(x_{t+1}, \xi_{t+1}\right) + \alpha E\left(V_{t+2}\left(x_{t+1}, \xi_{t+2}\right)\right) \tag{21}$$

At the initial iteration, the Monte Carlo Simulation (MCS) is performed without considering future cost values (cost-to-go estimation). This initial assumption is expressed as:

$$E\left(V_{t+1}\left(x_t\right)\right) = 0 \tag{22}$$

Subsequently, a backward pass is executed to compute an approximation of the cost-to-go function, which is

then used in the next forward pass iteration to improve decision-making. At the final stage of the time horizon, the expected future cost is assumed to be zero:

$$V_{T+1}\left(x_T\right) = 0 \tag{23}$$

During the forward pass, all distribution network and Battery Swapping Cabinet (BSC) operational constraints are incorporated to ensure feasible decision-making while optimizing power management and mitigating phase unbalance.

Upon completing the forward pass, the backward pass is initiated, starting from the final stage at t = T-1 and progressing backward to t = 1. This step estimates the cost-to-go function using linear regression. The dual variables, which capture the sensitivity of the cost function with respect to the charging power of the BSC, are derived from the optimization process. These dual variables are then utilized to construct a piecewise linear approximation of the future cost function, contributing to the formulation of a new cut βin the value function approximation.

$$\boldsymbol{B}_t^k \, x_t^k \;+\; \beta_t^k \;\leq\; \theta_{t+1}^k \tag{24}$$

where $\boldsymbol{B}_t^k$ is a matrix containing coefficients that represent the sensitivity of the cost function with respect to the charging power of the battery swapping cabinet (BSC) at time step t during the k-th iteration. These sensitivity values are estimated using:

$$\boldsymbol{B}_{i,t}^k = \frac{f^k\left(x_t^*, \xi_t\right) - f^k\left(x_t, \xi_t\right)}{\Delta x_{i,t}} \tag{25}$$

$\Delta x_{i,t}^k$ represents the change in decision variable at location i corresponding to the charging or discharging power of the BSC at time step t during the k-th iteration, θ_{t+1}^k denotes the approximated cost-to-go function at the next time step $t+1$ during the k-th iteration. It represents the expected future cost value based on current optimization decisions.

The SDDP algorithm iterates until convergence criteria are met. Convergence is determined by comparing the linear approximation of future cost function and the evaluated cost function, ensuring that the difference satisfies a predefined threshold:

$$\left|U\boldsymbol{B}^k - L\boldsymbol{B}^k\right| \leq \varepsilon \tag{26}$$

where ε is a small convergence threshold, $U\boldsymbol{B}^k$ is evaluated future cost at iteration k, given by:

$$U\boldsymbol{B}^k = min\, \boldsymbol{C}^k(x_2) \tag{27}$$

$L\boldsymbol{B}^k$ is peicewise linear approximation of future cost at iteration k, given by:

$$L\boldsymbol{B}^k = \mathrm{E}\left(\mathrm{V}_2\left(\mathrm{x}_1\right)\right)^k \tag{28}$$

To provide a clear representation of the proposed methodology, the following algorithm presents the structured implementation of the bi-level stochastic optimization framework adopted in this study. The upper level focuses on the strategic placement of Battery Swapping Cabinets (BSCs), guided by sensitivity analysis and network operation constraints, including loadability margin considerations, to ensure technical feasibility and to enhance phase balancing effectiveness. The lower level addresses the dynamic operational scheduling of the BSCs through the application of Stochastic Dual Dynamic Programming (SDDP), facilitating multi-stage decision-making under uncertainty. The algorithm detailed below encapsulates the principal computational procedures employed for the joint optimization of BSC placement and energy management.

The application of the bi-level stochastic optimization framework for the strategic placement and operational scheduling of Battery Swapping Cabinets (BSCs) to enhance phase balancing in low-voltage distribution networks under uncertainty is described as follows.

Input:

- Network data, including topology, bus parameters, load profiles, and line limits.
- BSC specifications: power capacity, slot capacity, and state-of-charge (SOC) limits.
- Probability distribution functions (PDFs) representing electricity consumption at each bus and EV battery swapping demand.
- Optimization parameters: number of scenarios (Ns), time horizon (T), and discount factor (α).

Begin:

Level 1: BSC Placement Optimization.

Step 1: Generate Ns stochastic scenarios of electricity demand using the probability distribution functions defined for each bus.

Step 2: For each scenario, apply the Differential Evolution (DE) optimization procedure:

- For each candidate bus i and potential phase connection:
  - Simulate a charging mode by increasing the load at bus i by 1 p.u.
  - Simulate a discharging mode by decreasing the load at bus i by 1 p.u.
  - Evaluate the corresponding voltage sensitivity and loadability margin, as described in Section 2.1.

Step 3: Identify, for each scenario, the set of bus-phase combinations that yield the highest sensitivity values while satisfying all network constraints.

Step 4: Evaluate the convergence of the Monte Carlo Simulation (MCS) to ensure stability in the placement results.

Level 2: BSC Operational Optimization Using SDDP

Step 5: For each BSC location determined in Level 1, initialize the SOC of all batteries b in each BSC for all time steps t.

Step 6: Repeat until convergence:

a. Forward Pass (for t = 1 to T):

For each time step t and each scenario ξ_t:

i Solve the operational optimization problem using the objective function and constraints described in Section 2 and Equations (20)–(23) in Section 3.3.
ii Store the optimal power exchange between the BSC and the grid, the selected operational phase, and the resulting SOC at the end of the time step.
b. Backward Pass (for $t = T$ to 1):
i Approximate the cost-to-go function using the results of the forward pass by summing the objective values from time $t + 1$ to T.
ii Estimate the sensitivity of the cost function with respect to the BSC charging power, following Equation (25).
iii Update the cuts to satisfy the cost-to-go condition expressed in Equation (24).
iv Incorporate these sensitivities and cuts into the next iteration's forward pass to improve future cost approximations.
v Evaluate the convergence of the SDDP.

Output:
- Optimal BSC placement (bus locations).
- Time-varying charging and discharging schedules for each BSC and phase of connections.
- Quantitative improvements in voltage unbalance factor (VUF) and neutral line power losses.

4. SIMULATION AND RESULTS

This study utilizes a 104-bus LV distribution network located in north-eastern (NE) Thailand, as depicted in Figure 2. The network, operated by the Provincial Electricity Authority (PEA), functions at a voltage level of 400/230V and has a total load demand of 160.38 kW. The load is distributed across the three phases as follows 56.6 kW on phase A, 52.82 kW on phase B, and 50.97 kW on phase C, each operating with a lagging power factor of 0.85, as detailed in Figure 3. The minimum voltage levels observed in the system are 0.9517 pu for phase A, 0.9792 pu for phase B, and 0.9364 pu for phase C.

4.1 Optimal BSCs Placement

The simulation utilizes 2023 PEA-NE2 data [21] to analyze variations in electricity consumption. The dataset consists of 15-minute interval demand data and includes multiple consumer categories, such as small residential (SR) consumers with monthly consumption below 150 units, large residential (LR) consumers exceeding 150 units, and small general service (SGS) consumers. The demand data for each category, as well as their combinations, has been statistically analyzed and fitted to appropriate probability distribution functions (PDFs), as illustrated in Figure 4. These fitted distributions are then applied to represent demand variations in the test network, as detailed in Table 1.

Photovoltaic (PV) systems in the test network are modelled as customer-installed units with the capability to deliver power to the grid. In this study, 10 kW single-phase PV systems are strategically placed at phase

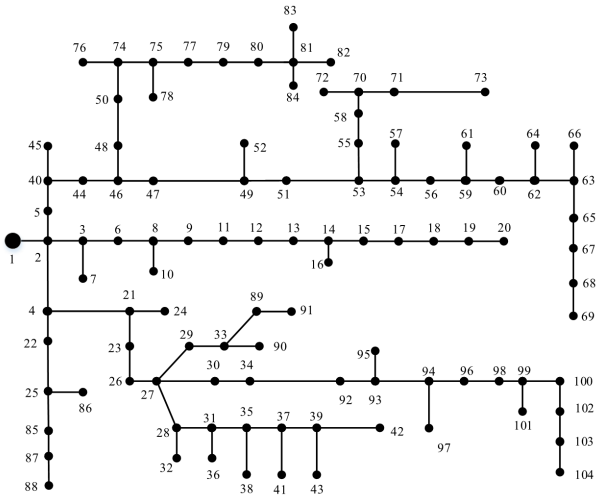

***Fig. 2**: PEA 104-bus LV Distribution Network.*

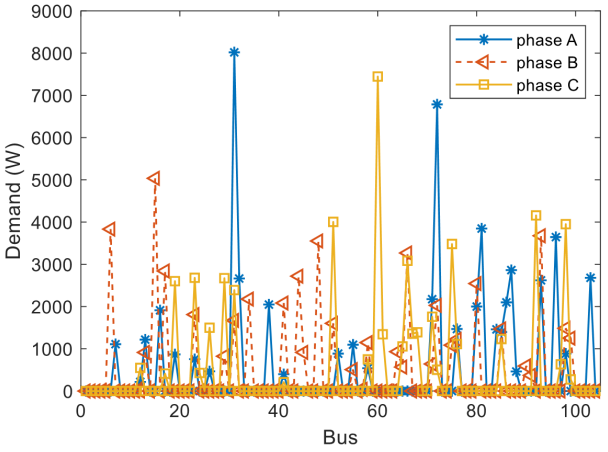

***Fig. 3**: Electricity Demand.*

A of bus 31, phase B of bus 15, and phase C of bus 60, representing realistic deployment scenarios in north-eastern Thailand.

As depicted in Figure 5, the normalized probability distribution of PV output exhibits a mean generation of 0.48 kW, with a skewness of -0.04, kurtosis of 1.75, and standard deviation of 0.3 kW. Analysis reveals that when PV systems deliver power at their mean output level, the base case Voltage Unbalance Factor (VUF) of the network reaches 2.44%, while neutral line losses decrease to 0.4169 pu. These findings indicate that PV generation alters power flow dynamics, affecting VUF and neutral line losses, while simultaneously increasing the uncertainty of network operation due to its variable and intermittent nature.

The battery swapping cabinets (BSCs) are strategically positioned in three designated zones: Zone 1 serves the area covering buses 2 to 43, Zone 2 covers buses 44 to 84, and Zone 3 spans buses 85 to 104. The results reveal that buses 17, 66, and 99 emerge as the most frequent and optimal locations for both charging and discharging operations, ensuring efficient energy

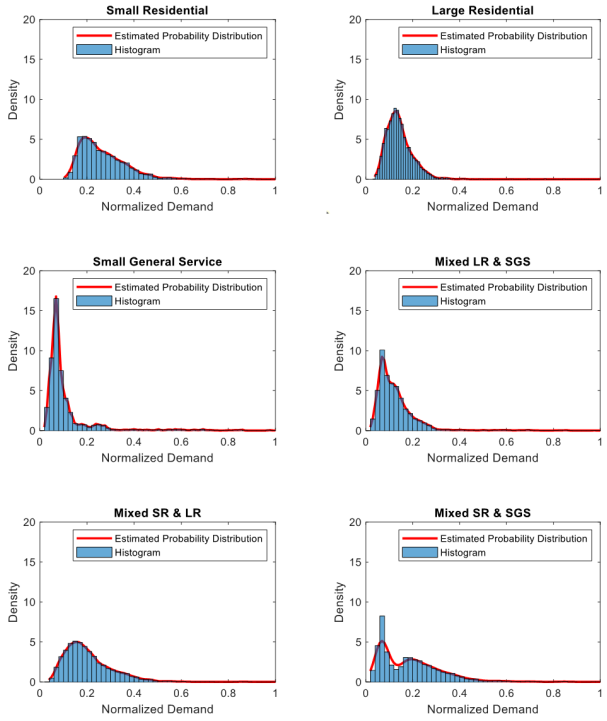

***Fig. 4**: Probability Distribution of Each Demand Category.*

***Table 1**: Demand Characteristics for Test Network.*

Bus number	Phase A	Phase B	Phase C
1 - 20	LR	Mixed SR & LR	SR
21 – 40	SR	LR	Mixed SR & LR
41 – 60	SR	SGS	Mixed LR & SGS
61 – 80	SGS	Mixed SR & SGS	LR
81 - 104	Mixed SR & SGS	SR	SGS

distribution and enhanced phase balancing within the network. As illustrated in Figure 6, these locations exhibit high-frequency selection in the optimization process, confirming their suitability for maximizing grid stability.

Figure 6 illustrates the frequency of optimal BSC placements, highlighting the differences in the spatial distribution of charging and discharging locations. The results indicate that charging operations are more concentrated, with fewer buses identified as optimal locations, while discharging operations are more widely distributed across multiple buses. Since many low-frequency discharging solutions were identified during the optimization process, only the most frequently selected locations are shown in the figure to maintain clarity and focus on the most significant placements. The optimization was conducted using 500 Monte Carlo Simulation (MCS) scenarios, allowing for robust evaluation under varying demand conditions. The approach achieved a Standard Error of the Mean (SEM) below 0.01, ensuring a high degree of reliability in the placement results.

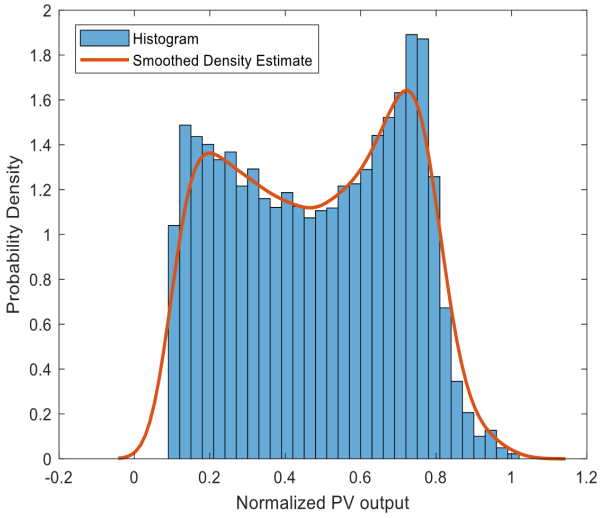

***Fig. 5**: Normalized Distribution of PV System Output.*

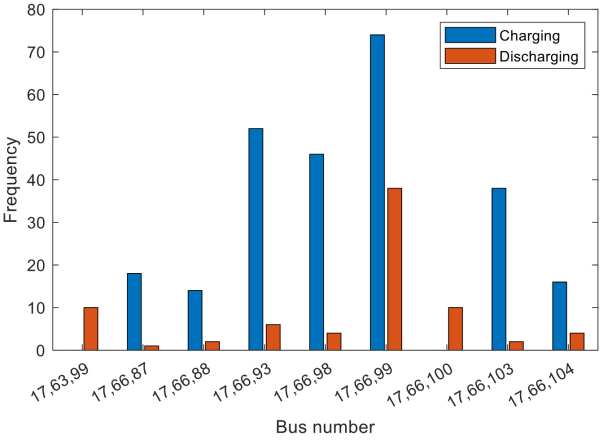

***Fig. 6**: Optimal Placement of the BSCs.*

For cases involving the deployment of existing BSC infrastructure, this location selection process can be bypassed, allowing direct implementation of stochastic dynamic programming for energy management.

4.2 Energy Management

This study examines 24 time-intervals within a single day, focusing on hourly fluctuations in electrical load demand. This approach was chosen over 15-minute intervals, which result in 96 time periods per day and significantly increase the complexity of the problem as the number of intervals grows [22]. To facilitate analysis, the 15-minute interval demand data from the PEA-NE2 region were aggregated into hourly averages. The aggregated data were then statistically analysed and fitted to appropriate probability distribution functions (PDFs) for each hour of the day, providing a realistic

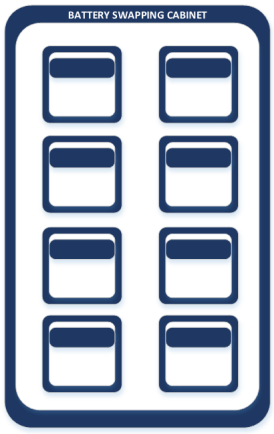

Number of bin	8
Input Voltage	100~240VAC
Frequency	50Hz
Max power	6200W
Max power per bin	900W
Battery Voltage	48V/60V/72V

***Fig. 7**: BSC Specifications and Characteristics.*

representation of stochastic demand behaviour.

Demand imbalance has been identified as a significant factor contributing to phase unbalance in the distribution network. To account for the uncertainties associated with load variations, 100 scenarios were generated and analysed to evaluate the role of BSCs in mitigating phase unbalance. The BSC model considered in this study features an 8-slot battery swapping cabinet, a commercially available solution designed specifically for electric motorbike batteries, as depicted in Figure 7. This 8-slot cabinet supports 48V, 60V, and 72V lithium-ion batteries, with a single-phase input voltage ranging from 100–240 VAC at 50 Hz, a maximum power rating of 6200 W, and a maximum power output per slot of 900 W. The integration of this BSC configuration into the distribution network enables efficient energy management while addressing phase imbalance conditions.

The demand for BSC services is classified into three time periods: peak, partial-peak, and off-peak. Typically, the highest demand occurs during the morning commute and evening post-work hours. However, additional demand from food delivery riders is expected to increase BSC usage from late morning to early afternoon and in the evening. Unlike household plug-in electric vehicles PEVs, where the probability of initiating charging is highest around 6 PM, leading to a peak in EV load at approximately 8 PM [23], the charging demand from battery swapping cabinets varies based on service schedules rather than fixed residential charging patterns. Table 2 provides a detailed classification of EV service demand across different time periods and specifies the number of reserved battery packs required for each demand level.

A leading company in the electric scooter market has established an extensive battery-swapping network, with operational data indicating an average battery swap frequency of five to six swaps per hour *[24]*. Based on this data, the reserved battery count in this study is set at five packs during off-peak periods, eight packs during mid-peak periods, and twelve packs during peak periods. The arrival of EVs for battery swapping at the BSC is assumed to follow a Poisson distribution, with a mean

***Table 2**: Classification of BSC Service Demand Periods.*

Time Period (hrs)	Demand Category	Reserved battery packs (units)
07:00 – 08:00, 15.00 – 16.00	Partial-peak	8
11:00 – 14:00, 17:00 - 21:00	Peak	12
others	Off-peak	5

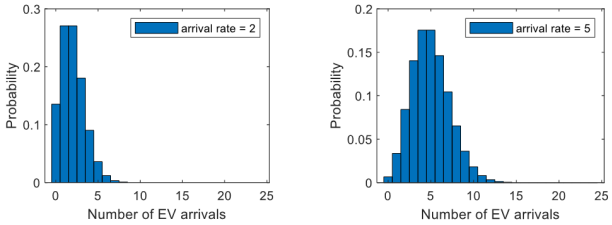

***Fig. 8**: Probability Distribution of EV Arrivals.*

arrival rate of two vehicles per hour during off-peak periods, five during mid-peak periods, and eight during peak periods. The probability distribution of EV service demand is illustrated in Figure 8.

Building on the operational model described above, each installation location is assumed to have two BSC stations, providing a total capacity of 16 battery packs. The reserved battery requirements are set proportionally to the total capacity, with approximately 30 percent reserved during off-peak periods, 50 percent during mid-peak periods, and 75 percent during peak periods to ensure sufficient availability for EV services.

The batteries considered in this study have a voltage rating of 72V, a capacity of 30 Ah, and a rated power of 2160Wh, with standard charging currents of 0.5C or 1C. The maximum allowable charging current is 2C; however, the BSC slot limits the charging and discharging currents. At maximum slot power, the charging current is restricted to 0.42C. Operating at maximum power for 1 hour delivers 900Wh of energy, equivalent to 41.68% of the battery's SoC.

In this study, the depth of discharge (DoD) for lithium-ion batteries is set at 80%, meaning discharging is only allowed until the SoC reaches 20%. To support phase unbalance mitigation, battery packs with lower SoC are prioritized for discharging, ensuring faster recharging when needed for EV service. Conversely, batteries with higher SoC are prioritized for charging to maximize the availability of fully charged units. Under normal conditions, charging is limited to 90% SoC, but if required for phase unbalance mitigation, batteries may charge up to 100%. When an EV uses the BSC service, a fully charged battery replaces a depleted one, with the swapped battery's SoC following a normal distribution between 10% and 30%.

The simulation begins with an initial state that corresponds to the SoC of the batteries, as shown in

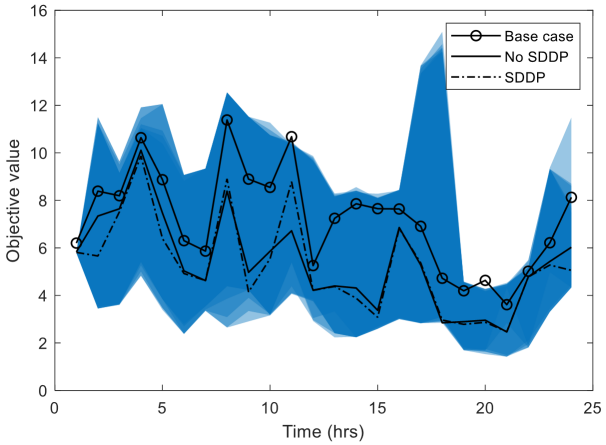

***Fig. 9**: Objective Value Variation over a 24-hour Time Horizon.*

Figures 11a – 13a at time step 1. SDDP is performed with 100 scenarios per time step, where the upper and lower bounds of the objective function are represented by the shaded area in Figure 9, with increasing shading intensity as the iterations progress. To ensure a balance between short-term and long-term decision-making, a discounting factor of 0.95 is applied when estimating the cost-to-go in the forward pass of SDDP.

If future variations in electricity demand and EV battery swapping demand align with the predicted pattern shown in Figure 8, the system's objective value evolution over a 24-hour horizon is illustrated in Figure 9. The Base case, represented by the line with circular markers, reflects system operation without any deployment of BSCs, resulting in higher and more volatile objective values. Under a myopic strategy, where BSC charging power is optimized solely based on the immediate system state, the optimal power compensation follows a rigid trajectory, represented by the solid black line. However, when SDDP is applied, the power allocation adapts dynamically to fluctuating demand conditions, as indicated by the dashed black line in Figure 9.

The impact of this adaptive decision-making framework is profound. Without SDDP, the future cost of the system stands at 124.01, whereas with its application, this cost drops to 120.32, achieving a 2.97% reduction through intelligent, scenario-based optimization, the SDDP approach leads to noticeable alterations in the phase connection and operational mode of the BSCs as shown in Figure 10. These adjustments reflect the algorithm's ability to dynamically reallocate power flows across phases and time to better accommodate demand uncertainties and minimize system imbalance. Moreover, the SDDP framework converges efficiently within just 7 iterations, reinforcing its effectiveness in guiding optimal power management strategies (Figure 14).

The influence of BSC deployment on network stability is even more striking. Without BSC integration, the objective value for network unbalance mitigation over the analysed time horizon reaches 173.05. However, with strategic BSC placement and operation, this value is slashed by 30.47%, showcasing the pivotal role of BSCs in mitigating phase unbalance and improving distribution network resilience. This remarkable improvement highlights the transformative potential of BSC-based energy management, making it a game-changer for modern low-voltage networks.

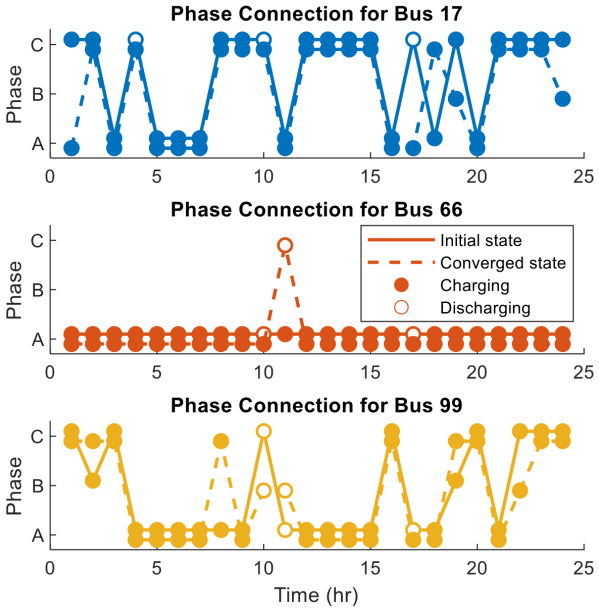

***Fig. 10**: Phase Connection and Operational Mode.*

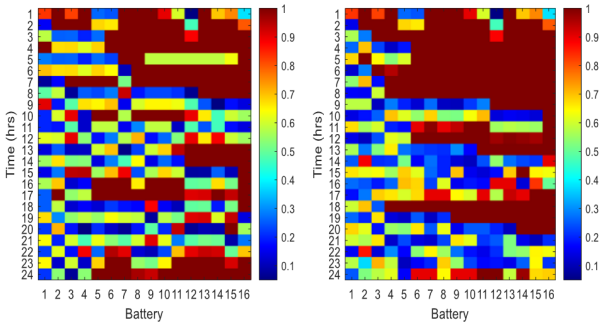

***Fig. 11**: SoC at Bus 17 a) Initial State b) Converged State.*

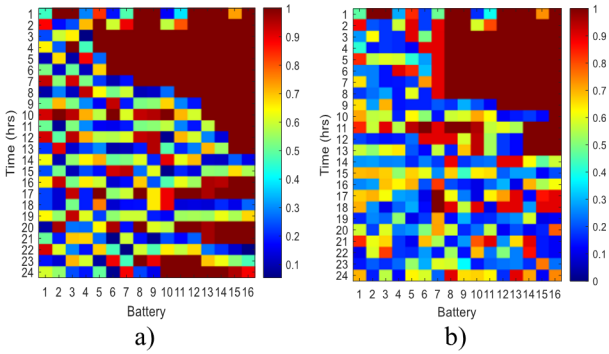

***Fig. 12**: SoC at Bus 66 a) Initial State b) Converged State.*

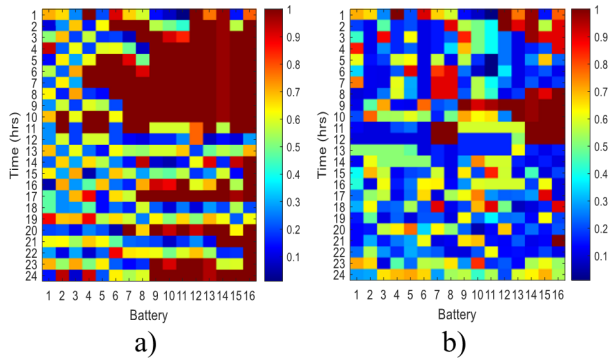

***Fig. 13**: SoC at Bus 99 a) Initial State b) Converged State.*

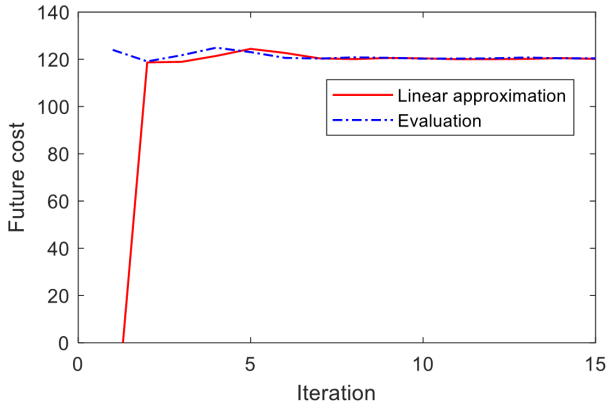

***Fig. 14**: Convergence of SDDP.*

The evolution of battery SoC throughout the optimization process unveils the transformative impact of the BSC's energy management strategy. Figures 11–13a illustrate the initial SoC distribution across different locations, while Figures 11–13b capture the post-optimization state, showcasing the refined energy allocation achieved through SDDP.

These shifts in SoC levels are not just numerical adjustments—they represent the intelligent adaptation of BSC operations, striking a delicate balance between ensuring sufficient battery availability for EV services and actively contributing to phase unbalance mitigation in the distribution network. The strategic power management executed by BSCs reshapes the charging landscape, optimizing energy utilization while reinforcing grid stability.

To maintain precision in tracking energy flow and cost optimization, charging and discharging efficiencies (η_c and η_d) are standardized at 1 during SoC evaluations. This ensures a consistent and transparent assessment of energy transitions, reinforcing the effectiveness of the proposed optimization framework in orchestrating seamless power distribution across the network.

5. DISCUSSION

This study demonstrates the effectiveness of battery swapping cabinets (BSCs) in addressing phase unbalance and optimizing power distribution in low-voltage networks with increasing electric vehicle (EV) adoption. Traditional approaches to mitigating phase imbalance often require network reconfiguration or infrastructure modifications, which can be costly and disruptive. In contrast, the strategic deployment of BSCs offers a flexible and efficient solution that dynamically manages charging loads, reducing the Voltage Unbalance Factor (VUF) by up to 30.47%.

A key insight from this research is that BSCs predominantly function in charging mode, with limited occurrences of discharging due to operational constraints and service demand. Despite this, their intelligent scheduling still plays a crucial role in balancing single-phase loads and reducing neutral current. The stochastic optimization approach, which integrates Stochastic Dual Dynamic Programming (SDDP) with Monte Carlo Simulation (MCS), enables the system to adapt to fluctuations in EV charging demand and household electricity consumption. This adaptability ensures a more stable and predictable network operation.

Another significant outcome is the impact of network uncertainty on optimization performance. Variability in EV arrival times and charging demand necessitates a robust decision-making framework that can accommodate real-time fluctuations. The study reveals that a myopic strategy, which considers only the present state without anticipating future variations, results in less effective phase balancing. By incorporating future cost estimations and iterative learning, the SDDP-based approach achieves a 2.97% reduction in overall system cost, demonstrating its capability to guide proactive energy management.

This research primarily focuses on the technical aspects of deploying BSCs to enhance network stability and power quality. However, an important consideration for future work is the economic dimension of BSC operations. A comprehensive framework should account for the financial interests of both BSC service providers and utility operators, ensuring that system improvements align with economic feasibility. Future studies could explore dynamic pricing models, financial incentives for optimized charging schedules, and energy trading mechanisms between BSC owners and grid operators. These additions would not only enhance phase balancing but also create a financially sustainable model for integrating BSCs into distribution networks.

Although the results confirm the benefits of BSCs in improving network stability, some challenges remain. The inability of BSCs to discharge energy in certain scenarios suggests that additional mechanisms, such as coordination with distributed energy resources (DERs) or demand response strategies, may be required. Additionally, interactions between BSC operations and other grid components, such as photovoltaic (PV) systems, introduce further complexities that must be addressed for holistic power flow optimization.

Overall, the findings highlight the feasibility of using

BSCs as an effective tool for enhancing power quality and mitigating voltage unbalance in distribution systems. The proposed optimization framework provides a scalable approach to integrating BSCs while maintaining operational efficiency. Moving forward, incorporating economic factors into the decision-making process will be essential to ensure that both network operators and BSC service providers achieve mutually beneficial outcomes in the evolving energy landscape.

6. CONCLUSION

This study presents a novel approach to deploying BSCs as a dual-purpose solution for battery charging and phase balancing in low-voltage distribution networks. A sensitivity-based optimization framework strategically places BSCs to mitigate phase imbalance while supporting battery-swapping operations. A loadability margin constraint ensures power absorption and delivery remain within operational limits. To account for uncertainties in EV battery swapping demand and household energy consumption, a stochastic optimization framework combining SDDP and MCS is implemented. This enables real-time adaptability, optimizing power distribution and maintaining grid reliability. Additionally, a coordinated energy management strategy aligns utility operators and BSC service providers to enhance network efficiency and stability.

The findings highlight BSCs as a scalable and practical solution for phase balancing in evolving power grids. By strategically integrating BSCs, this study advances network stability while laying the groundwork for future research on economic optimization and cost-effective deployment strategies. These insights contribute to the development of smart-grid-compatible EV infrastructure, positioning BSCs as a critical component in next-generation power distribution systems.

REFERENCES

[1] K. Girigoudar and L. A. Roald, "On the impact of different voltage unbalance metrics in distribution system optimization," *Electric Power Systems Research*, vol. 189, p. 106656, 2020.

[2] A. A. R. Mohamed, R. J. Best, D. J. Morrow, A. Cupples, and I. Bailie, "Impact of the deployment of solar photovoltaic and electrical vehicle on the low voltage unbalanced networks and the role of battery energy storage systems," *Journal of Energy Storage*, vol. 42, p. 102975, 2021.

[3] M. R. Islam, H. Lu, M. J. Hossain, and L. Li, "Mitigating unbalance using distributed network reconfiguration techniques in distributed power generation grids with services for electric vehicles: A review," *Journal of Cleaner Production*, vol. 239, p. 117932, 2019.

[4] H. Shi, H. Xiong, W. Gan, Y. Lin, and C. Guo, "Fully distributed planning method for coordinated distribution and urban transportation networks considering three-phase unbalance mitigation," *Applied Energy*, vol. 377, p. 124449, 2025.

[5] S. T. Siddharthan and A. Shunmugalatha, "A Robust approach for mitigating load voltage imbalances using glowworm swarm optimizer for power quality enrichment," *Electric Power Systems Research*, vol. 229, p. 110101, 2024.

[6] M. Vanin, T. Van Acker, H. Ergun, R. D'hulst, K. Vanthournout, and D. Van Hertem, "Congestion mitigation in unbalanced residential networks with OPF-based demand management," *Sustainable Energy, Grids and Networks*, vol. 32, p. 100936, 2022.

[7] K. Yufeng, "60% of food delivery riders in Singapore signed up during Covid-19 pandemic: Survey".

[8] Y. Lin, R. K. Marjerison, J. Choi, and C. Chae, "Supply chain sustainability during COVID-19: Last mile food delivery in China," *Sustainability*, vol. 14, no. 3, p. 1484, 2022.

[9] A. Tabares and P. Cortés, "Using Stochastic Dual Dynamic Programming to Solve the Multi-Stage Energy Management Problem in Microgrids," *Energies*, vol. 17, no. 11, p. 2628, 2024.

[10] A. Kiszka and D. Wozabal, "Stochastic dual dynamic programming for optimal power flow problems under uncertainty," *European Journal of Operational Research*, vol. 321, no. 3, pp. 814–836, 2025.

[11] R. M. Ciric, A. P. Feltrin, and L. F. Ochoa, "Power flow in four-wire distribution networks-general approach," *IEEE Transactions on Power Systems*, vol. 18, no. 4, pp. 1283–1290, 2003.

[12] P. S. Kundur, N. J. Balu, and M. G. Lauby, "Power system dynamics and stability," *Power system stability and control*, vol. 3, pp. 700–701, 2017.

[13] M. Niu, N. Z. Xu, H. N. Dong, Y. Y. Ge, Y. T. Liu, and H. T. Ngin, "Adaptive range composite differential evolution for fast optimal reactive power dispatch," *IEEE Access*, vol. 9, pp. 20117–20126, 2021.

[14] K. V. Price, "Differential Evolution," in Handbook of Optimization, vol. 38, I. Zelinka, V. Snášel, and A. Abraham, Eds., in Intelligent Systems Reference Library, vol. 38. , Berlin, Heidelberg: Springer Berlin Heidelberg, 2013, pp. 187–214. doi: 10.1007/978-3-642-30504-7_8.

[15] X.-S. Yang and X. He, "Swarm Intelligence and Evolutionary Computation: Overview and Analysis," in Recent Advances in Swarm Intelligence and Evolutionary Computation, vol. 585, X.-S. Yang, Ed., in Studies in Computational Intelligence, vol. 585. , Cham: Springer International Publishing, 2015, pp. 1–23. doi: 10.1007/978-3-319-13826-8_1.

[16] S. Khunkitti, A. Siritaratiwat, and S. Premrudeepreechacharn, "A many-objective marine predators algorithm for solving many-objective optimal power flow problem," *Applied Sciences*, vol. 12, no. 22, p. 11829, 2022.

[17] R. Y. Rubinstein and D. P. Kroese, Simulation and the Monte Carlo method. John Wiley & Sons, 2016.
[18] G. Lan, "Complexity of stochastic dual dynamic programming," *Mathematical Programming*, vol. 191, no. 2, pp. 717–754, 2022.
[19] O. Mégel, J. L. Mathieu, and G. Andersson, "Stochastic dual dynamic programming to schedule energy storage units providing multiple services," in *2015 IEEE Eindhoven PowerTech*, IEEE, 2015, pp. 1–6.
[20] X. Xi, R. Sioshansi, and V. Marano, "A stochastic dynamic programming model for co-optimization of distributed energy storage," *Energy Systems*, vol. 5, pp. 475–505, 2014.
[21] "Load Profile :: Load Research of PEA." Accessed: Aug. 08, 2024. [Online]. Available: http://peaoc.pea.co.th/loadprofile/en/
[22] A. Shapiro, "On complexity of multistage stochastic programs," *Operations Research Letters*, vol. 34, no. 1, pp. 1–8, 2006.
[23] B. Azzopardi and Y. Gabdullin, "Impacts of Electric Vehicles Charging in Low-Voltage Distribution Networks: A Case Study in Malta," *Energies*, vol. 17, no. 2, p. 289, 2024.
[24] "Impact - Gogoro." Accessed: Feb. 12, 2025. [Online]. Available: https://investor.gogoro.com/impact/

Bongkoj Sookananta is an Assistant Professor in the Department of Electrical and Electronics Engineering at Ubon Ratchathani University, Thailand. She earned her Ph.D. in Electrical Engineering from the University of Strathclyde, UK. Her research focuses on optimization and artificial intelligence in electrical power systems, with particular interests in electric vehicles, energy storage, renewable energy resources, and uncertainty in power system operations. Her work plays a crucial role in advancing sustainable and efficient energy solutions for modern power networks.

Mongkol Pusayatanont is an Assistant Professor in the Department of Electrical and Electronics Engineering at Ubon Ratchathani University, Thailand. He holds a Ph.D. in Electrical Engineering from the University of Sussex, United Kingdom. His research focuses on condition monitoring in process control, flow measurement, motor drives, renewable energy resources and AC machines. Dr. Pusayatanont's work significantly contributes to advancements in motor drive hardware and signal monitoring within drive systems.